Equilibrium mean charge states for low-Z ions at ≤ 1 MeV/u in carbon

Chris Schmitt,[1] Jay LaVerne,[1,2,*] Daniel Robertson,[1] Matthew Bowers,[1] Wenting Lu,[1] and Philippe Collon[1]
[1]*Department of Physics, University of Notre Dame, Notre Dame, Indiana 46556, USA*
[2]*Radiation Laboratory, University of Notre Dame, Notre Dame, Indiana 46556, USA*
(Received 29 September 2009; published 25 November 2009)

Equilibrium mean charge states have been measured for 3–7 MeV lithium, boron, and carbon ions passing through thin carbon foils. The data are compared to the predictions of several semiempirical models of charge equilibrium in the ≤ 1 MeV/u regime. The current work underscores the general problem of extrapolating models developed for high-Z projectiles to ions of low Z. A compilation of experimental data for low-Z ions in the low-energy regime has been used to reparametrize a few of the charge equilibrium models. Experimental techniques, comments and suggestions on the nature of the equilibrium charge states of low-Z ions are presented.

DOI: 10.1103/PhysRevA.80.052711 PACS number(s): 34.70.+e

I. INTRODUCTION

Fast ions lose energy by Coulombic interactions with the electrons of a medium so knowledge of the charge state of the ion is essential to describing a number of fundamental properties including the stopping power of the medium and the range of the ions. [1] Radiation effects and dosimetry are two of many areas that are ultimately dependent on the charge state of the incident ion. Applications of importance range from accelerator design and accelerator mass spectrometry to medical therapy. Unfortunately, significant gaps exist in the data for the charge distribution of low-energy ions in solid materials, which makes it difficult to determine the trustworthiness of stopping power and range compilations.

Fast ions traversing a medium will undergo a series of electron capture and loss collisions. If the medium is thick enough then an ample number of collisions will occur to establish an equilibrium charge state distribution. Various experimental studies have been performed using a variety of ion and target combinations covering a wide range of energies. Several reviews and tables have accumulated the data for equilibrium charge state distributions for Be, B, and C ions using carbon foils [1–6]. Lithium ion equilibrium charge state distributions have been reported by Itoh [7] in the energy range of 1–6 MeV and by Stocker and Berkowitz [8] in the energy range of 5.8–16.4 MeV. Equilibrium charge state distributions for He ions have been reported by Armstrong. [9] Thin carbon foils of well-known thicknesses are relatively simple to make and easy to use. Therefore, equilibrium charge state distributions in carbon foils are important because of its common use as a standard for comparison between experiments and with established models.

In this work, equilibrium charge state distribution measurements have been performed for lithium, boron and carbon ions emerging from a carbon foil in the energy range of 3–7 MeV. A comparison with experimental literature values has been made to establish the accuracy of the techniques used for these studies. The combined experimental data has been compared to the predictions of a variety of semiempirical formalisms to show their suitability and range of application. In addition, beam detection techniques are discussed and shown that they can be useful in this kind of experiment. Comments and suggestions on the nature of the equilibrium charge state distributions of low-Z ions are presented.

II. EXPERIMENTAL PROCEDURE

A variety of experimental procedures for measuring the charge fraction of ions passing through thin foils have been employed and the current work has adapted a technique similar to that used by Ishihara *et al.* [10] Low-Z ions are produced by a Source of Negative Ions by Cesium Sputtering negative-ion source and accelerated by the FN Tandem Van de Graaff in the Nuclear Structure Laboratory at the University of Notre Dame. The incident ions pass through the accelerator mass spectrometry (AMS) beamline and through a carbon foil in the scattering chamber. The scattering chamber has a moveable target ladder that holds three foil targets, a Faraday cup (FC), and an empty frame to allow passage of the bare beam (see Fig. 1). Some of the ion beam is Rutherford scattered into a silicon (monitor) detector located in the scattering chamber, which acts as an ion-beam monitor and a normalization tool. The unscattered beam is sent directly into a Browne-Buechner spectrograph where the charge state fractions are separated magnetically and measured by an electron suppressed FC. The spectrograph FC is mounted on a set of rails referred to as the "zero degree rails" as shown in Fig. 1. Previous papers have been published by this group that details the experimental facilities, the beamline, and properties of the spectrograph [11,12].

All of the ions are magnetically selected to give ions of well defined energy initially in the 2+ charge state. Passage of the ions through a carbon foil results in an equilibrium distribution of charge states (Li: 1+ to 3+, B: 1+ to 5+, and C: 1+ to 6+). The spectrograph magnet is carefully scanned to bring each of the charge states onto the FC and the identity of each charge state is then verified through the following scaling procedure:

$$\vec{B} \propto I_{magnet} \propto 1/q,$$

where $\vec{B}$ is the magnetic field of the spectrograph, I_{magnet} is the current supplied to the spectrograph magnet and q is the

*Corresponding author; laverne.1@nd.edu

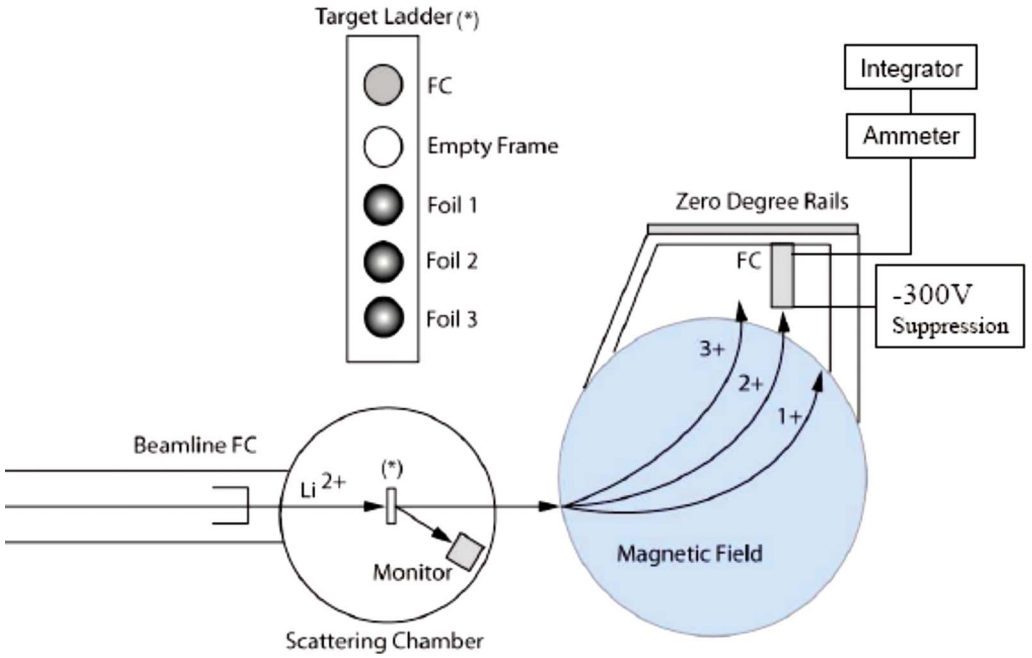

FIG. 1. (Color online) Schematic of the experimental setup specific for measuring charge state fractions. For a full overview of the entire AMS beamline see Refs. [11,12]. The (*) indicates the target ladder and its general makeup, the silicon monitor detector in relation to the foils and the FC mount on the zero degree rails.

charge state. With the charge state distribution mapped the next step is to bring the first charge state back onto the FC and maximize the current by adjusting the magnetic field. Then three to five full charge state scans are taken while measuring the integrated current on the FC and the scattered beam on the monitor detector to check reproducibility. Once the first charge state has been measured then the next charge state is moved onto the FC and the procedure is repeated. When a charge state distribution for a given energy has been measured the charge fractions can be calculated using $F_q = N_q / \Sigma N_q$, where F_q is the charge fraction and N_q is $N_q = I_q / qeW$ with I_q being the current read from the FC, q is the charge state, e is 1.6×10^{-19} C, and W is the normalization counts from the monitor. Following the determination of the charge fractions, the mean charge can be determined using $\bar{q} = \Sigma q F_q$ and the distribution width, $d = [\Sigma (q - \bar{q})^2 F_q]^{1/2}$, can also be calculated. This procedure is repeated for multiple ions and energies.

Energy loss through the foil should be negligible so as to not influence the measurements of the charge fractions. The SRIM2008 program by Ziegler [13] suggests that lithium of 3–7 MeV will have an energy-loss range of approximately 43–60 keV for a 20-μg cm^{-2}-thick carbon foil. Boron[1] and carbon ions at 3–6 MeV will lose approximately 110–118 and 143–146 keV, respectively, in a carbon foil of the same thickness. These expected energy loses are too small to significantly change the incident ion energy and thereby affect the charge state distribution. Estimated errors as based on statistics of counts and reproducibility of the repeated measurements are on the order of a few percent or less.

[1] ^{10}B was used and then scaled to ^{11}B to compare with established data.

III. RESULTS AND DISCUSSION

A. Comparison with literature data

Since the present configuration has never been used to measure charge state distributions a direct comparison with literature values in carbon foils was first performed. Figure 2 shows the present results for lithium ions with the data for lithium ions by Itoh. [7] Also shown in Fig. 2 are the present results for boron and carbon ions with carbon ion data by Shima [5]. The agreement between the sets of data for lithium, boron and carbon ions is excellent, which indicates

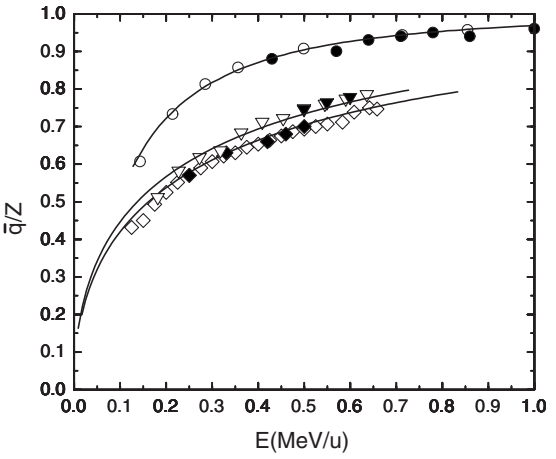

FIG. 2. Variation in the relative ionization as a function of the incident energy for lithium ions from Itoh [7] (open circles) and current work (closed circles) compared to the Itoh model and similarly for boron and carbon ions from Ref. [5] (open inverted triangles, diamond, respectively) and the current work (closed inverted triangles, diamond, respectively) using the To-Drouin model.

TABLE I. Experimental mean charge states and distribution widths of lithium, boron, and carbon.

^{7}Li	Incident energy (MeV)	$\bar{q}$	d	^{11}B	Incident energy (MeV)	$\bar{q}$	d	^{12}C	Incident energy (MeV)	$\bar{q}$	d
	3	2.65	0.48		5.5	3.73	0.64		3	3.39	0.65
	4	2.70	0.46		6.05	3.82	0.64		4	3.78	0.68
	4.5	2.78	0.44		6.6	3.89	0.65		5	3.96	0.58
	5	2.83	0.40						5.5	4.09	0.63
	5.5	2.86	0.30						6	4.18	0.63
	6	2.83	0.38								
	7	2.89	0.32								

that the present technique is trustworthy. The differences between the different sets of measurements are estimated to be less than one percent. A model developed by Itoh for the prediction of the mean charge state for lithium ions gives excellent agreement to the data as shown in Fig. 2, where deviations are due to beam fluctuations. A slightly different model for higher Z ions was developed by To-Drouin for boron and carbon, but was tested with ions up to argon [14]. The predictions of the latter model are seen in Fig. 2 to agree well with the boron and carbon ion data. Table I summarizes the experimental mean charge states for each ion species at the incident ion energy examined by this group. In all cases, the mean charge state increases monotonically with increasing ion energy. Ions of lower energy could not be examined because of instabilities in the beam transport.

B. Comparison with established semiempirical models

A variety of semiempirical models have been developed to predict the experimental mean charge state. These models were usually constructed from data for a limited number of ions and targets and were optimized over a finite-energy range. The following three formulas are examined in more detail because they were designed to fit the low-energy range covered in this work. In all the models, the relative ionization $(\bar{q}/Z)$ is given. This quantity is defined as the mean charge state of the ion divided by its Z.

The To-Drouin model was specifically developed for application to the range of ions from boron to argon and the relative ionization is represented as

$$\bar{q} = Z[1 - \exp(-X)], \tag{1}$$

where the reduced velocity is $X = 3.86Z^{-0.45}\sqrt{E[\mathrm{MeV}]/M[\mathrm{amu}]}$ [7] and is limited by $0.2 \leq X \leq 1.6$ and $5 \leq Z \leq 18$ [14].

A formula created by Schiwietz *et al.* [15,16] is a highly parametrized least-squares fit built from an array of over 800 data points that span a wide variety of ions and targets. The expression for the relative ionization is given as

$$\bar{q} = Z\left[\frac{(8.29x + x^4)}{0.06/x + 4 + 7.4x + x^4}\right], \tag{2}$$

where

$$x = c_1(\tilde{v}/c_2/1.54)^{1+1.83/Z}, \tag{3}$$

is a reformulated reduced velocity and the power term is used to adjust the steepness of the charge state curves as a function of x with the following correction terms:

$$c_1 = 1 - 0.26e^{-Z_t/11}e^{-(Z_t - Z)^2/9} \quad \text{and} \quad c_2 = 1 + 0.030\tilde{v}\ \ln(Z_t). \tag{4}$$

The first term accounts for resonant electron capture, which reduces the mean charge state or similarly x for symmetrical ion-target combinations, while the second correction term allows for a target dependent deformation at high velocities. The final component in the reformulated reduced velocity is the scaled projectile velocity

$$\tilde{v} = Z^{-0.543}v_p/v_B. \tag{5}$$

The sub- and superscripts have "p" for projectile, "B" for Bohr, and "t" for target. The limitations noted for this model are that the ratio of the projectile velocity to the Bohr velocity for protons and helium must be greater than 2 and for all other ions the ratio must be greater than 0.4.

The last expression to be examined here is the Ziegler, Biersack, and Littmark model that is used in the well-known SRIM and TRIM codes. The expression for He ions is given as

$$\gamma^2 = 1 - \exp\left[-\sum_{i=0}^{5} a_i \ln(E)^i\right], \tag{6}$$

where γ is defined as the fractional effective charge of the ion, a_i are fitting constants that were determined to be $a_0 = 0.2865$, $a_1 = 0.1266$, $a_2 = -0.001\,429$, $a_3 = 0.024\,02$, $a_4 = -0.011\,35$, and $a_5 = 0.001\,75$ and E is in units of keV/amu. This equation can be written into a form similar in notation to the other semiempirical expressions used in this work,

$$\bar{q} \approx Z\left\{1 - \exp\left[-\sum_{i=0}^{5} a_i \ln(E)^i\right]\right\}^{1/2}. \tag{6a}$$

The fractional effective charge γ is approximately equal to the relative ionization $(\bar{q}/Z)$ based on the definition of effective charge, $q_{eff} = Z\gamma$. Some assumptions that are made for the derivation of Eq. (6) include that the effective ion charge is independent of target material and that the effective ion charge of H is always unity.

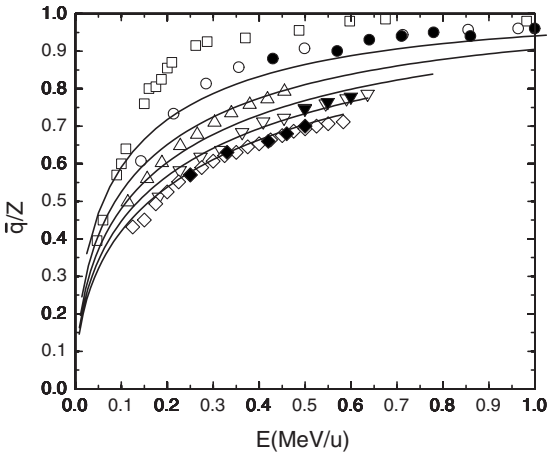

FIG. 3. Variation in the relative ionization as a function of initial ion energy for the To-Drouin model (solid lines), He ions (squares) [9], Li ions (circles) [7], Be ions (triangles) [5], B ions (inverted triangles) [5], and C ions (diamonds) [5]. Closed data points are from this work and open ones are from the literature.

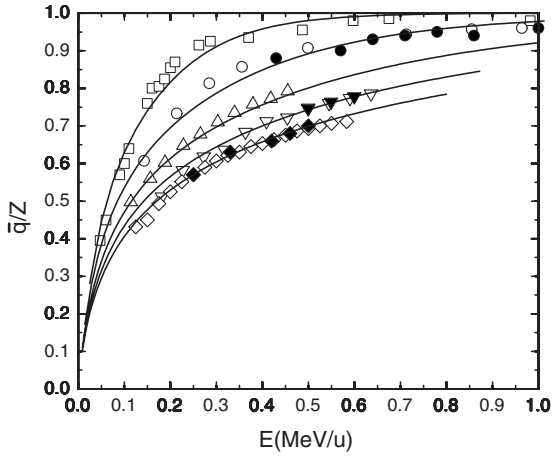

FIG. 4. Variation in the relative ionization as a function of initial ion energy for the Schiwietz model (solid lines), He ions (squares) [9], Li ions (circles) [7], Be ions (triangles) [5], B ions (inverted triangles) [5], and C ions (diamonds) [5]. Closed data points are from this work and open ones are from the literature.

For ions of Z greater than 2 the Ziegler, Biersack, and Littmark formula can be written as

$$\bar{q} = Z[1 - \exp(0.803y_r^{0.3} - 1.3167y_r^{0.6} - 0.381\,557y_r - 0.008\,983y_r^3)], \tag{6b}$$

where y_r is the reduced velocity as given by $\frac{v_r}{v_B Z^{2/3}}$ and v_r is the relative velocity as given by

$$v_r = v\left(1 + \frac{v_F^2}{5v^2}\right) \tag{7}$$

for $v > v_F$ and

$$v_r = \frac{3v_F}{4}\left(1 + \frac{2v^2}{3v_F^2} - \frac{v^4}{15v_F^4}\right) \tag{8}$$

for $v \leq v_F$ [13] where v is ion velocity and v_F is the Fermi velocity of the medium.

Experimental charge state distributions for Li, B, and C ions are presented with the three model predictions in Figs. 3–5 where the relative ionization is given as a function of incident energy per amu. The figures readily show how well the data, current and older, compare with the To-Drouin, Schiwietz, and Ziegler-Biersack-Littmark models, respectively. The comparison is quantified by examining the percent deviation between the experimental values and the calculated ones.

The To-Drouin model works best with the higher Z ions such as B and C. Huge deviations are observed between this model and data with the lighter Z ions. For example, the worst case is with He ions, where the deviation is as large as 17%. The deviation decreases to about 12% with Li ions and to about 5.1% for Be ions. Even with B and C ions, the deviation of 8% is the greatest at the lowest energy and less than 3% at higher energies. The To-Drouin model clearly struggles with ions of low Z and it is not very accurate with any light ion at low energy.

The comparison of the Schiwietz model with the experimental data, Fig. 4, shows a reasonably good fit with the data for every ion especially those with Z below that of B ions. The maximum deviations between model predictions and the data are $<3.1\%$ with He ions, $<4.5\%$ with Li ions and $<1.8\%$ with Be ions. As observed with the To-Drouin model, the largest deviations with B and C ions are at the lowest energies with 3 and 6% deviation, respectively. The higher energy B and C ions have deviations of less than 3% and 2%, respectively.

The Ziegler-Biersack-Littmark model predictions for all of the ions other than He are within 9% of the data. The general trend of the model is to give larger deviations at lower energies and better agreement with the data as the energy increases. Except at the lowest energies, the Schiwietz model reproduces the data very well and it seems to be

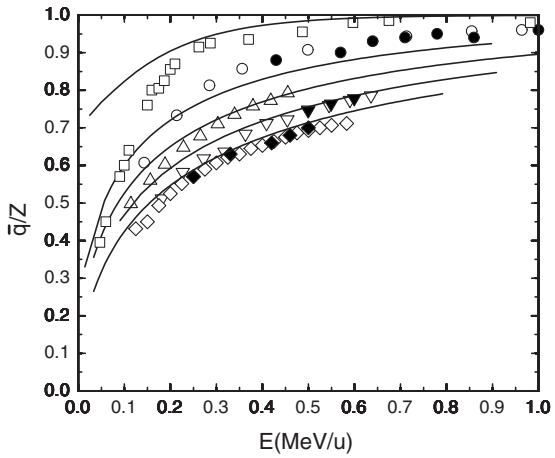

FIG. 5. Variation in the relative ionization as a function of initial ion energy for the Ziegler-Biersack-Littmark model (solid lines), He ions (squares) [9], Li ions (circles) [7], Be ions (triangles) [5], B ions (inverted triangles) [5], and C ions (diamonds) [5]. Closed data points are from this work and open ones are from the literature.

the best of the three models in this regime. With increasing Z, the To-Drouin model starts to close the gap with the Schiwietz model, but the upper bound on the To-Drouin model is argon ions whereas the Schiwietz model has been tested with ions of much larger Z. In general, all the models seem to improve with increasing energy.

None of models examined here specifically addresses the shell effects that have been reported with Z and Z_2 oscillations [17]. These shell effects originate with the electronic structure of the projectile ion and include the ability of the target atom to be an electron sink or reservoir. An example of this shell effect is as follows, when bromine ions are stripped in solids near 140 MeV the mean charge reaches 25 and remains relatively constant at lower energies [4]. Further ionization requires removal of L electrons from the ion. However, those electrons are more tightly bound and the probability of removing them becomes small in comparison to lower-energy M electrons. This kind of behavior leads to oscillatory structure instead of smooth trends in the relative ionization as a function of energy. The observation of this type of data is an indicator for some of the underlying physics in charge equilibrium.

There seems to be a systematic deviation between model predictions and the data that is more prominent at lowers energies. In the higher energy regime the ions are fully stripped or are protonlike projectiles where shell effects have become negligible and the relative ionization ($\bar{q}/Z$) becomes Z independent. A compensation Z (ion)-dependent term to allow for shell effects in the low-energy region has been proposed in addition to the standard X value presented in the semiempirical models for the mean charge state or relative ionization [7].

The parametrizations of some of the models for the prediction of the mean charge state have suffered from the lack of systematic data. The use of only a few data points can lead to oversimplification and erroneous extrapolation to other Z ions or different energy regimes. On the other hand, there has been a general trend to look at massive pools of data to build a master expression that covers everything. This approach often misses potential underlying structure. Figure 6(a) shows the relative ionization of carbon ions emerging from a carbon foil over the energy range of 0–5 MeV/u. The figure contains three sets of data that give what looks like a relatively smooth variation in charge as a function of energy. However, examination of the data over a smaller energy range such as 0–1 MeV/u as in Fig. 6(b) gives a different view of the data. The solid line drawn in Fig. 6 is there to guide the eyes and shows a distinctive step behavior. All three sets of data that are shown have the same response, which strongly suggests that this effect is real and repeatable.

The approach to the fitting of data in Fig. 6(a) is commonly used to achieve a global fit of the data. Such a global model is built with the intention of covering of wide array of ions, target materials, and energy but at the loss of accuracy in some energy regimes. The question now arises as to how a local model compares to the best of the global models. A local model would give an expression that covers a smaller range of energies and a specific ion-target combination. There are several regression fits that can be used to build such a local model. The following section explores several approaches and present arguments on the physicality of such choices.

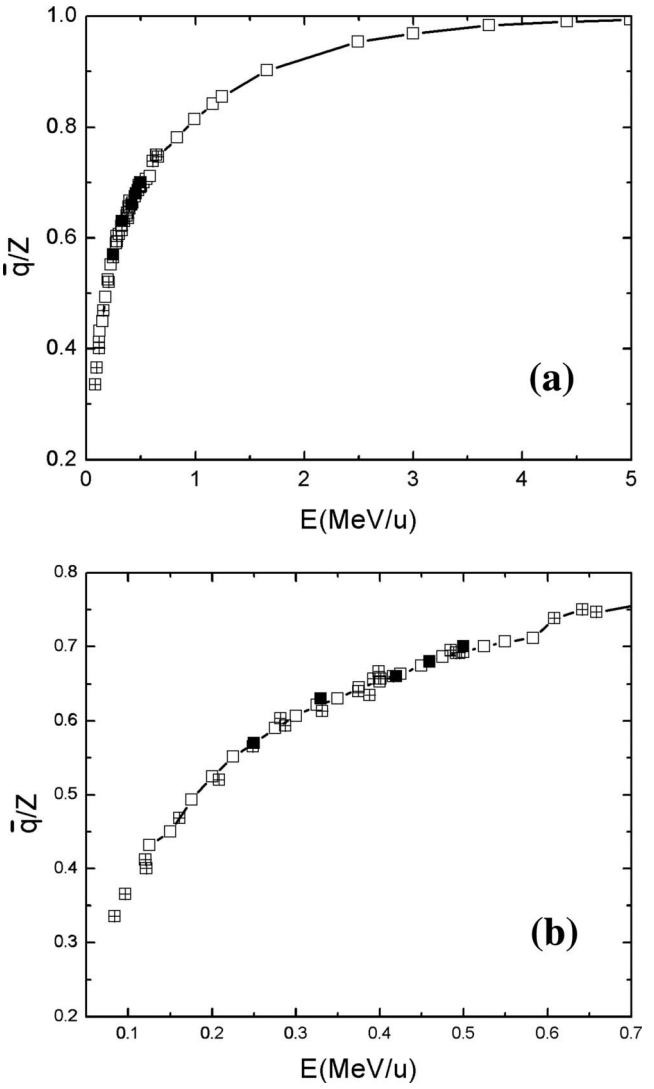

FIG. 6. The relative ionization of carbon ions through carbon foils for an energy range from (a) 0–5 MeV/u and (b) 0–0.7 MeV/u (b). The line through the data points is to guide the eyes. Open squares are from Ref. [4]. Closed squares are current data. Open squares with a plus are from Ref. [5].

C. Development of local models

Most semiempirical relative ionization models (global and local) are built based on the work of Betz who in turn used a suggestion from Heckman *et al.* to focus on $\ln(1-\bar{q}/Z)$, which represents the mean relative number of electrons carried by the ions, as a function of a reduced velocity [18,19]. Following a simple rearrangement, the relative ionization can take the form of $\bar{q}=Z[1-T\exp(-\frac{v}{v_\beta Z^\gamma})]$, where T and γ are determined empirically and v is the ion velocity and v_β is the Bohr velocity. The quantity inside the parentheses is readily identified as the reduced velocity.

The general trend of the experimental data is that the mean charge state increases uniformly (monotonically) with

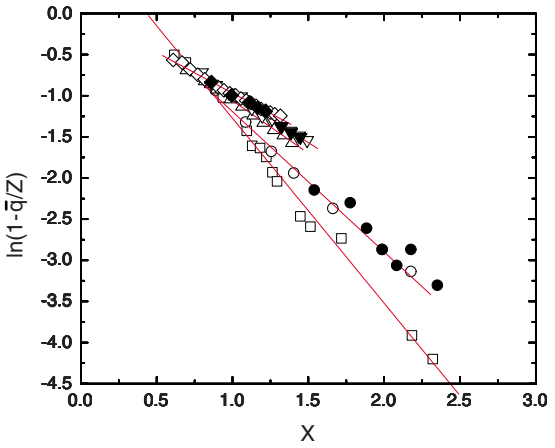

FIG. 7. (Color online) Fit of the parameter $\ln(1-\bar{q}/Z)$ as a function of the linear coordinate X (solid lines) with He ions (squares) [9], Li ions (circles) [7], Be ions (triangles) [5], Be ions (inverted triangles) [5], and C ions (diamonds) [5]. Closed symbols are this work and open symbols are from the literature.

energy, which suggests a linear function as a valid choice. The form of the regression fit will take the form of $AX+B$ where A is the slope and B is the y-intercept in the linear relationship. The mean charge will take the form of $\bar{q}=Z[1-\exp(AX+B)]$. A second regression fit that will be examined here is a third-order polynomial fit in which the mean charge will take the form of $\bar{q}=Z[1-\exp(CX^3+DX^2+EX)]$ where the y intercept is set to zero to mimic the look of the model developed by Shima-Ishihara-Mikumo [5,6].

Due the apparent linear nature of the relative ionization data and models in the literature, a linear regression fit was the logical choice in developing a good local model. The values for $\ln(1-\bar{q}/Z)$ as a function of the reduced velocity, X, are shown in Figs. 7 and 8 for the five ion species through a carbon target. The resulting coefficients are displayed in Tables II and III with the corresponding R^2 values, which describe statistically how well the regression fits to the data. A R^2 value of 1 is considered a perfect fit.

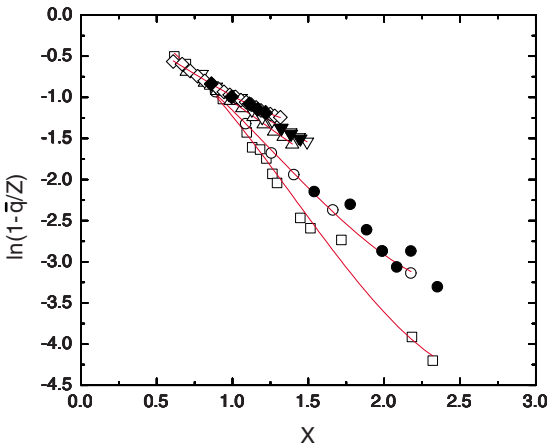

FIG. 8. (Color online) Fit of the parameter $\ln(1-\bar{q}/Z)$ as a function of the polynomial coordinate X (solid lines) with He ions (squares) [9], Li ions (circles) [7], Be ions (triangles) [5], (inverted triangles) [5], and C ions (diamonds) [5]. Closed symbols are this work and open symbols are from the literature.

TABLE II. The coefficients and R^2 values related to linear fits.

	A	B	R^2
He	−2.2469	0.9731	0.9914
Li	−1.7038	0.5112	0.9956
Be	−1.2787	0.2195	0.9992
B	−1.1764	0.1951	0.9937
C	−0.9866	0.0195	0.9929

The linear fits for He and Li ions in Fig. 7 fit well enough with the lines either going through the data points or just grazing them, while Be and higher Z ions seem to be well represented with linear functions. With the development of a functional fit a balance of attaining the highest R^2 value must be tempered with a little bit of physics. For example, as $X \rightarrow 0$ so does $\bar{q}/Z$ and the expression must have a y intercept of zero. The fits to the data of Fig. 7 clearly show that the best regressions have nonzero intercepts, which potentially leads to unrealistic physics as $X \rightarrow 0$. Forcing a zero y intercept on the linear fits creates an equally poor situation where the fit does not conform to the data. The results suggest that despite a linear trend in the data higher order terms are needed.

Third-order polynomial fits of the data are given in Fig. 8. The rational for this type of functional dependence is based on the model of Shima-Ishihara-Mikumo, but the energy ranges of that model are not applicable to the current work [5,6]. The R^2 values for the polynomial fits are slightly better than the linear fits. Statistically, both regression fits are close enough to be interchangeable, but the third-order polynomial fit has no y intercept to give more realistic physics.

Does a better fit always imply the correct physics? The argument could be made that until enough information is collected the best fit would be the more correct approach. It should be noted that the Itoh model has a nonzero y intercept, but as stated in Ref. [7] one of its limitations is the very low-energy regime. The physics of charge equilibrium in the very low-energy regime appears to be different than in the swift velocity regime. Low energies lead to a more quasimolecular state being prevalent and energy loss through the medium is dominated by nuclear interactions. Perhaps the nonzero y intercept term mimics some of the underlying physics, but the problem persists as to the nature of that physics and how to quantify it correctly in future mathematical fits. There has been some theoretical work with density-functional for-

TABLE III. The coefficients and R^2 values related to third-order polynomial fits.

	C	D	E	R^2
He	0.4825	−2.0204	0.3054	0.9924
Li	0.3697	−1.4065	−0.1225	0.999
Be	0.1242	−0.4737	−0.7054	0.9995
B	0.3373	−0.9413	−0.3793	0.995
C	0.4214	−0.858	−0.5474	0.9982

malisms exploring the very low-energy regime that lends some credence to the need of a y-intercept term [20].

The expectation is that a local model should provide a better fit than a global model because the regression fits are not weighed down by a large pool of data in various energy regimes. A more accurate model with respect to the variation in incident ions can be obtained when the target medium remains the same. As noted earlier, this approach clearly provides the advantage of observing potential underlying structure.

IV. CONCLUSION

Experimental observations for charge fraction measurements of Li, B, and C ions on carbon targets are found to be in excellent agreement with established data for the energy range examined. Comparison of the data with models that were developed for the energy range examined here shows that these models are not very accurate at very low energies. Of the three models examined, the Schiwietz model clearly shows the best response for lower energy of low-Z ions. The Schiwietz model follows one of the suggestions by Itoh *et al.* and includes a Z dependence. None of the models presented here for determination of mean charge take into account atomic phenomena such as shell structure and oscillation effects that have been reported by Shima [17]. The nature of the Z dependence in this energy range should continue to be explored with these same projectiles, but to include a systematic study of energy ranges as well as other target material.

ACKNOWLEDGMENTS

The authors would like to give special thanks to Larry Lamm for all of his technical assistance before, during, and after the experiment. This work was supported by the National Science Foundation (Grant No. NSF-PHY07-58110). The work of J.A.L. was supported by the Office of Basic Energy Sciences of the U.S. Department of Energy and this document is NDRL-4825 of the Notre Dame Radiation Laboratory.

[1] N. Bohr, K. Dan. Vidensk. Selsk. Mat. Fys. Medd. **18**, 1-144 (1948).
[2] S. K. Allison, Rev. Mod. Phys. **30**, 1137 (1958).
[3] H. D. Betz, Rev. Mod. Phys. **44**, 465 (1972).
[4] A. B. Wittkower and H. D. Betz, At. Data **5**, 113 (1973).
[5] K. Shima, T. Mikumo, and H. Tawara, At. Data Nucl. Data Tables **34**, 357 (1986).
[6] K. Shima, N. Kuno, and M. Yamanouchi, At. Data Nucl. Data Tables **51**, 173 (1992).
[7] A. Itoh, H. Tsuchida, T. Majima, A. Yogo, and A. Ogawa, Nucl. Instrum. Methods Phys. Res. B **159**, 22 (1999).
[8] H. Stocker and E. H. Berkowitz, Can. J. Phys. **49**, 480 (1971).
[9] J. C. Armstrong, J. V. Mullendore, W. R. Harris, and J. B. Marion, Proc. Phys. Soc. London **86**, 1283 (1965).
[10] T. Ishihara *et al.*, Nucl. Instrum. Methods **204**, 235 (1982).
[11] D. Robertson *et al.*, Nucl. Instrum. Methods Phys. Res. B **266**, 3481 (2008).
[12] D. Robertson *et al.*, Nucl. Instrum. Methods Phys. Res. B **259**, 669 (2007).
[13] J. F. Ziegler, J. P. Biersack, and U. Littmark, *The Stopping and Range of Ions in Solids* (Pergamon Press, New York, 1985).
[14] Ky Xuan To and R. Drouin, Nucl. Instrum. Methods **160**, 461 (1979).
[15] G. Schiwietz and P. L. Grande, Nucl. Instrum. Methods Phys. Res. B **175-177**, 125 (2001).
[16] G. Schiwietz, K. Czerski, M. Roth, F. Staufenbiel, and P. L. Grande. Nucl. Instrum. Methods Phys. Res. B **226**, 683 (2004).
[17] K. Shima, N. Kuno, T. Kakita, and M. Yamanouchi, Phys. Rev. A **39**, 4316 (1989).
[18] H. D. Betz, G. Hortig, E. Leischner, Ch. Schmelzer, B. Stadler, and J. Weihrauch, Phys. Lett. **22**, 643 (1966).
[19] H. H. Heckman, E. L. Hubbard, and W. G. Simon, Phys. Rev. **129**, 1240 (1963).
[20] N. Barberan and P. M. Echenique, J. Phys. B **19**, L81 (1986).